Optimized spatial frequency response in silver halide sensitized gelatin

A. Fimia, I. Pascual, and A. Beléndez

The authors are with Departamento Interuniversitario de Optica, Laboratorio de Optica, Universidad de Alicante, Apartado 99, Alicante E 03080, Spain. A. Beléndez is with the Departamento de Ingeniería de Sistemas y Comunicaciones, Universidad de Alicante.

Received 18 November 1991.
0003-6935/92/234625-03$05.00/0.

Silver halide sensitized gelatin processing is optimized to increase the spatial frequency response in Agfa-Gevaert 8E75 HD emulsion; therefore a diffraction efficiency of 55% in reflection gratings of 5000 lines/mm is achieved.

Key words: *Holography, holographic recording materials.*

One of the most important characteristics in the fabrication of high-efficiency, low-noise holographic optical elements is the spatial frequency response of the holographic recording materials. Dichromated gelatin (DCG) is a well-known recording material with high efficiency at high frequencies. On the other hand, silver halide sensitized gelatin (SHSG) is a process that improves the results in DCG (spectral and energetic sensitivity) and obtains a similar noise level.[1–5] When we use values of exposure that are similar to those used in SHSG, the DCG is sensitive only in the blue-green region of the spectrum.[6] It is possible to obtain diffraction gratings in DCG in the red zone. However, 200 times more energy[7] is needed to obtain these gratings than is needed when SHSG is used. As an example we have produced holographic lenses in SHSG that are 200 mm in diameter[8] by using a 15-mW He–Ne laser and an exposure time of 10 as a result of the energy sensitivity of the photographic emulsion. However, the SHSG spatial resolution is not high enough to produce reflection holographic optical elements[9] because of the limited resolution of the photographic emulsions employed in the photochemical process.

Basically the most important step in the photochemical processing of SHSG is the bleaching bath, because with this step the latent image is obtained. In the bleaching bath material transfer from the exposed areas to neighboring unexposed areas occurs. The mechanism that is responsible for this material transfer in such a bleaching bath contains not only an oxidizing agent and an alkali halide but usually also potassium bromide.[10] This excess produces an optimization in the local action of the Cr^{+3} ion.

On the other hand, the gelatin that supports the emulsion is important because of the hardening bias level achieved, which depends on the initial hardening of the gelatin. Thus an increase in the temperature of the bleach can modify the hardening bias level of the photographic emulsion.[11]

Graver *et al.*[12] have discussed the possible photochemical process that is produced by this process. However, there are some differences between the process presented by Graver and the method that we propose. First, he used a Kodak 649 F plate that has a type of gelatin that is different from the Agfa 8E75 HD plate that we used. This implies that the swelling factor is different.[11] Second, the bleaching agent used by Graver was R-9, while we used an R-10 rehalogenating bleach bath. According to our previous experimental results, if we eliminate the potassium bromide from the bleaching bath, the diffraction efficiency decreases significantly.

In this Technical Note we show that by using a Agfa 8E75 HD emulsion and a modified R-10 bleach, it is possible to obtain a 75% diffraction efficiency at a high spatial frequency (2000 lines/mm). We think that this is due to the potassium bromide content in this solution, which controls the average life span of the Cr^{+3} ions and therefore optimizes the action of the bleaching agent. Hariharan and Chidley[13] have addressed this issue of the effect of the bleaching agent, although he used different components in his bleaching solution.

To optimize and analyze SHSG the processing possibilities of unslated holographic transmission gratings between 600 and 2000 lines/mm were recorded on Agfa-Gevaert 8E75 HD plates, and the process that we followed was similar to that of Chang and Winick[1] but with the temperature of the bleaching bath modified to 50°C. Exposures were made at 633 nm by using an *s*-polarized He–Ne source.

After some trials we found that the diffraction efficiency increases significantly at high frequency by using the nonsolvent Kodak developer PAAP, which produces a better resolution than the D-19 developer. The curves in Fig. 1 show the variation of the maximum diffraction efficiency with the spatial frequency for the two developers.

Another significant improvement was discovered when the processing was stopped after bleaching. Plates were dried and maintained to 90% relative humidity in a dark room during a 24-h period pause [step (4) in Table 1]. As a result of this step the differential hardening is modified because we allow the darkening reaction to occur precisely in the areas in which the Cr^{+3} ion of the bleaching agent is used. The darkening reaction was reported in an earlier paper on DCG.[1] Thus the process was continued. In these trials we observed that the results depended on the atmospheric conditions in which the plate was stopped. One possible explanation for the increase in diffraction efficiency is that during the remainder of the time the trivalent chromium ion could form a great number of cross-link bonds. According to this hypothesis the high relative humidity would be favorable for cross-link formation, since the best results were obtained in this case.[14] In Fig. 2 we show how stopping the process in high-

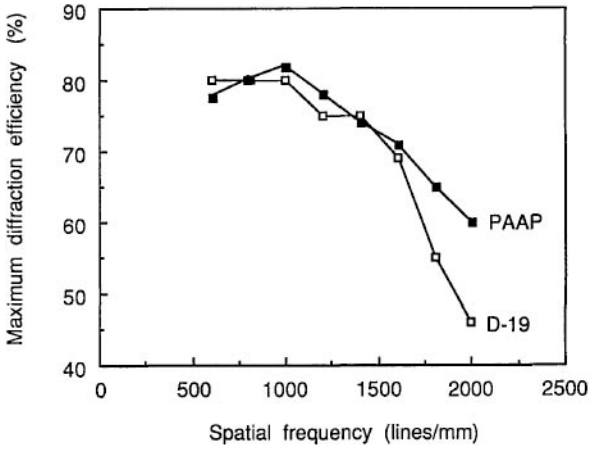

Fig. 1. Maximum diffraction efficiency as a function of the spatial frequency for unslated holographic transmission gratings developed with D-19 (□) and PAAP (■).

Table 1. Processing Schedule and Bleach Formula

Step:

(1) Develop with Kodak developer PAAP for 4 min.
(2) Rinse in running water for 1 min.
(3) Bleach in a modified R-10 solution for 30 s after the plate has cleared at 50°C (see the formula below).
(4) Stop at high humidity (90%) for 24 h.
(5) Rinse in running water for 30 s.
(6) Soak in fixer F-24 for 2 min.
(7) Wash in running water for 10 min.
(8) Dehydrate in 50% isopropanol for 3 min.
(9) Dehydrate in 90% isopropanol for 3 min.
(10) Dehydrate in 100% isopropanol for 3 min.
(11) Dry in vacuum chamber.

Note: All solutions are at 20°C except the bleaching step.

Bleach formula:

Solution A	
Distilled water	500 mL
Ammonium dichromate	20 g
Sulfuric acid	14 mL
Distilled water to make	1000 mL
Solution B	
Potassium bromide	92 g
Distilled water to make	1000 mL

Just before use, mix 1 part of A with 10 parts of distilled water, then add 30 parts of B.

humidity conditions affects the diffraction efficiency for holographic transmission gratings at a spatial frequency response of 2000 lines/mm when PAAP developer is being used. A comparison between the spatial frequency response for the PAAP developer with and without a stop in the process is shown in Fig. 3.

To confirm these results, diffraction gratings were recorded with two collimated beams of equal intensity illuminating the plates from opposite sides (reflection gratings). The angle between the two beams was 150° in the air, and the incidence of one of the beams on the plate was normal. Sets of gratings with the exposure varied were processed according to Table 1. Each grating was analyzed in an Oriel 7240 monochromator that maintained the recording geometry and varied the reconstructed wavelength to obtain maximum light intensity in the first diffracted order. The ratio of this light intensity to the incident intensity was taken as the diffraction efficiency of the grating. Since the average refractive index[15] of 8E75 HD emulsion is 1.64 at 633 nm, by using the geometry described we calculated the spatial frequency of the gratings to be 5000 lines/mm. Figure 4 shows the experimental results obtained for diffraction efficiency and reconstruction wavelengths as functions of the exposure for the holographic reflection gratings processed according to Table 1.

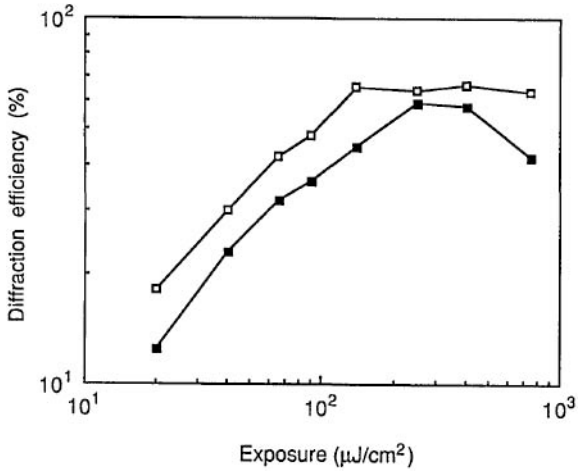

Fig. 2. Diffraction efficiency as a function of exposure for unslated holographic transmission gratings at a spatial frequency of 2000 lines/mm developed with PAAP with (□) and without (■) a stop in the processing.

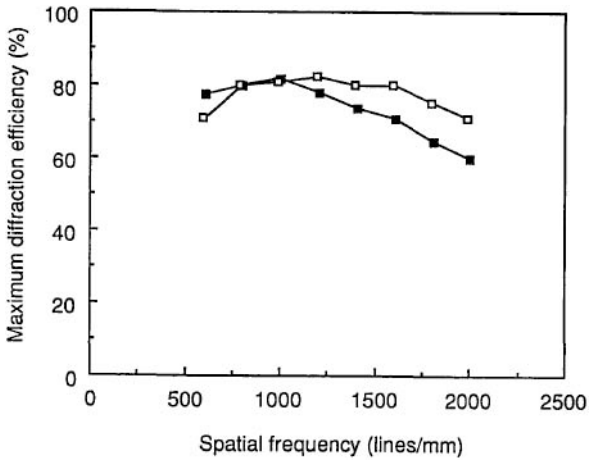

Fig. 3. Maximum diffraction efficiency as a function of spatial frequency for unslated holographic transmission gratings developed with PAAP with (□) and without (■) a stop in the processing.

As we can see from Fig. 4, it is possible to achieve a 55% diffraction efficiency. Moreover the reconstruction wavelength is lower than the recording wavelength since a lot of material is dissolved during the photochemical process. Both can be controlled in a wide range by adjusting the dichromate concentration and the acidity of the bleaching bath.[16] However, care must be taken because these changes can affect the diffraction efficiency. An alternative with organosilane coupling agents to adjust for the emulsion thickness variations has been proposed.[17]

In conclusion, the processing method that we have proposed and discussed here (Table 1) can optimize the spatial frequency response of SHSG. Thus a diffraction

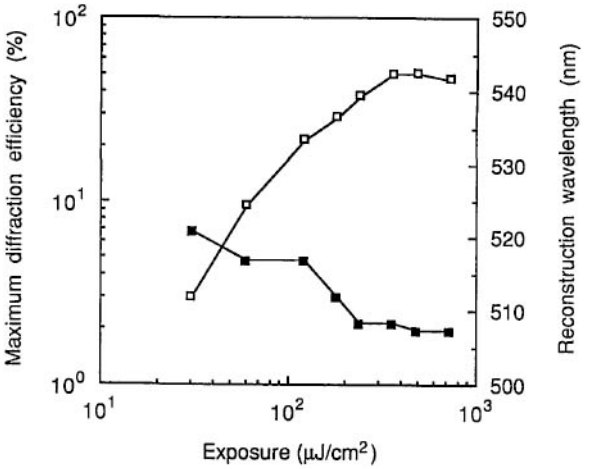

Fig. 4. Diffraction efficiency (□) and reconstruction wavelength (■) as functions of exposure for holographic reflection gratings processed according to Table 1.

efficiency of 55% is achieved by holographic reflection gratings of 5000 lines/mm with a suitable modification of the processing schedule, as has been proposed in previous papers. Finally, the results show the possibility of obtaining reflection gratings with a good level of diffraction efficiency in SHSG.

References

1. B. J. Chang and K. Winick, "Silver-halide gelatin holograms," in *Optical Alignment I,* R. N. Shagam and W. C. Sweatt, eds., Proc. Soc. Photo-Opt. Instrum. Eng. **251,** 172–177 (1980).
2. P. Hariharan, "Silver halide sensitized gelatin holograms: mechanism of hologram formation," Appl. Opt. **25,** 2040–2042 (1986).
3. A. Fimia, I. Pascual, C. Vázquez, and A. Beléndez, "Silver halide sensitized holograms and their applications," in *Holographic Optics II: Principles and Applications,* G. N. Morris, ed., Proc. Soc. Photo-Opt. Instrum. Eng. **1136,** 53–57 (1989).
4. A. Fimia, A. Beléndez, and I. Pascual, "Silver halide (sensitized) gelatin in Agfa-Gevaert plates: the optimized procedure," J. Mod. Opt. **38,** 2043–2051 (1991).
5. D. K. Angell, "Improved diffraction efficiency of silver halide (sensitized) gelatin," Appl. Opt. **26,** 4692–4702 (1986).
6. B. J. Chang and C. D. Leonard, "Dichromated gelatin for the fabrication of holographic optical elements," Appl. Opt. **18,** 2407–2417 (1979).
7. C. Solano, R. A. Lessard, and P. C. Roberge, "Red sensitivity of dichromated gelatin films," Appl. Opt. **24,** 1189–1192 (1985).
8. A. Beléndez, I. Pascual, and A. Fimia, "Holographic collimator of 200 mm diameter in silver halide sensitized gelatin," J. Opt. **21,** 211–215 (1990).
9. R. A. Ferrante, "Silver halide gelatin spatial frequency response," Appl. Opt. **23,** 4180–4181 (1984).
10. P. Hariharan, "Rehalogenating bleaches for photographic phase holograms. 3: Mechanism of material transfer," Appl. Opt. **29,** 2983–2985 (1990).
11. J. Oliva, P. J. Boj, and M. Pardo, "Dichromated gelatin holograms derived from Agfa 8E75 HD plates," Appl. Opt. **23,** 196 (1984).
12. W. R. Graver, J. W. Gladden, and J. W. Eastes, "Phase holograms formed by silver halide (sensitized) gelatin processing," Appl. Opt. **19,** 1529–1536 (1980).
13. P. Hariharan and C. M. Chidley, "Rehalogenating bleaches for photographic phase holograms: the influence of halide type and concentration on diffraction efficiency and scattering," Appl. Opt. **26,** 3895–3898 (1987).
14. J. Kosar, *Light-Sensitive Systems: Chemistry and Applications of Nonsilver Halide Photographic Processes* (Wiley, New York, 1965), Chap. 2.
15. R. K. Kostuk, "Factorial optimization of bleach constituents for silver halide holograms," Appl. Opt. **30,** 1611–1616 (1989).
16. J. Crespo, A. Fimia, and J. A. Quintana, "Fixation-free methods in bleached reflection holography," Appl. Opt. **25,** 1642–1645 (1986).
17. D. K. Angell, "Controlling emulsion thickness variations in silver halide (sensitized) gelatin," in *Holographic Optics: Design and Applications,* I. Cindrich, ed., Proc. Soc. Photo-Opt. Instrum. Eng. **883,** 106–113 (1988).

Nonlinear refractive index of IV–IV compound semiconductors

Richard A. Soref

The author is with the U.S. Air Force Rome Laboratory, Hanscom Air Force Base, Massachusetts 01731.

Received 6 February 1992.
0003-6935/92/234627-03$05.00/0.

An E_g^{-4} scaling law is used to estimate the intensity-dependent refractive index n_2 of the new binary zinc blende semiconductors GeC, β-SiC, SiGe, SnC, SiSn, and GeSn from known n_2 values for Si and Ge.

Nonlinear optical components in group-IV materials are needed to advance silicon-based optoelectronics. The second-order optical susceptibilities $\chi^{(2)}$ of ordered cubic IV–IV materials were estimated recently,[1] and the purpose of this Note is to extend the analysis to the third-order susceptibility $\chi^{(3)}$. The intensity-dependent index of refraction n_2 is related to $\chi^{(3)}$ in centimeter-gram-second units by $n_2 = (2\pi/n_0)\mathrm{Re}[\chi^{(3)}]$, where n_0 is the linear refractive index. Estimates of n_2 are presented here for the new cubic materials GeC, SnC, SiGe, SiSn, and GeSn (which have not yet been grown) and for β-SiC, Si, Ge, and C. An E_g^{-4} scaling law is used with the experimental n_2 values for Si and Ge.

This Note addresses the fast bound-electron nonlinearity, which is also called the valence-electron or virtual-state nonlinearity. Two-photon absorption is the primary mechanism for this nonlinearity, and the photon energy $\hbar\omega$ in this case is within the transparent region of the semiconductor: $\hbar\omega < E_i$, where E_i is the indirect band gap to the X_1 or L_1 conduction-band minima of the group-IV material. Stronger nonlinearities are also present, as discussed below.

The scaling law introduced by Sheik-Bahae *et al.*[2] was found to be successful in predicting the n_2 behavior for a wide variety of semiconductors and insulators, although only one group-IV material was checked against the theory. The rule is n_2 (esu) $= K'G_2/(n_0E_g^4)$, where K' is a constant, E_g is the minimum valence-to-conduction band gap, G_2 is a dimensionless dispersion function of $\hbar\omega/E_g$ that reaches a maximum at $\hbar\omega = E_g/2$, and n_0 is the linear index at $\hbar\omega < 0.5E_g$.

To apply the scaling rule to group-IV materials, we need to know the direct and indirect band gaps (E_d and E_i) as well as n_0. However, E_d, E_i, n_0, and the cubic-lattice parameter a have never been measured for the $\bar{4}3m$ crystals GeC, SnC, SiGe, SiSn, and GeSn. Therefore we made a series of estimates, as follows. The cubic-lattice constant (Table 1) was estimated for alloy AB by using Vegard's law: $a(\mathrm{AB}) = (1/2)[a(\mathrm{A}) + a(\mathrm{B})]$. Next we plotted E_i and E_d (listed in Table 1) as a function of a for the known materials C, β-SiC, Si, and Ge with the result shown in Fig. 1. Here E_d is the vertical separation at the zone center from the top of the highest valence band to the bottom of the lowest conduction band. The known indexes n_0 for C, β-SiC, Si, and Ge are listed in Table 1. Reference 3 discusses the estimation of n_0 from the oscillator model $n_0^2 - 1 = \Omega^2/E_{\mathrm{eff}}^2$, which gives a linear index of 2.68 for GeC, 3.85 for SnC, and 3.71 for SiGe. The dielectric model $\epsilon_r = n_0^2$ of Ref. 1 gives n_0 of 4.24 for SiSn and 4.47 for GeSn.

Moss' rule $n_0^4E_g = 77$ eV is valid for a range of II–VI and III–V semiconductors. By analogy with this rule, we took the known n_0 and the known band gaps for C, β-SiC, Si, and Ge to make a plot of $n_0^4\,E_i$ and $n_0^4\,E_d$ as a function of lattice spacing, with line segments connecting the experimental points for linear interpolation. The results, shown in Fig.